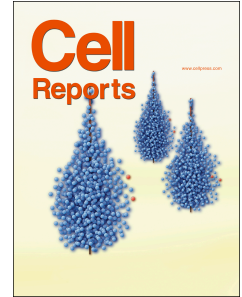


Journal Pre-proof



Major role of IgM in the neutralizing activity of convalescent plasma against SARS-CoV-2

Romain Gasser, Marc Cloutier, Jérémie Prévost, Corby Fink, Éric Ducas, Shilei Ding, Nathalie Dussault, Patricia Landry, Tony Tremblay, Audrey Laforce-Lavoie, Antoine Lewin, Guillaume Beaudoin-Bussièrès, Annemarie Laumaea, Halima Medjahed, Catherine Larochelle, Jonathan Richard, Gregory A. Dekaban, Jimmy D. Dikeakos, Renée Bazin, Andrés Finzi

PII: S2211-1247(21)00104-2

DOI: <https://doi.org/10.1016/j.celrep.2021.108790>

Reference: CELREP 108790

To appear in: *Cell Reports*

Received Date: 19 October 2020

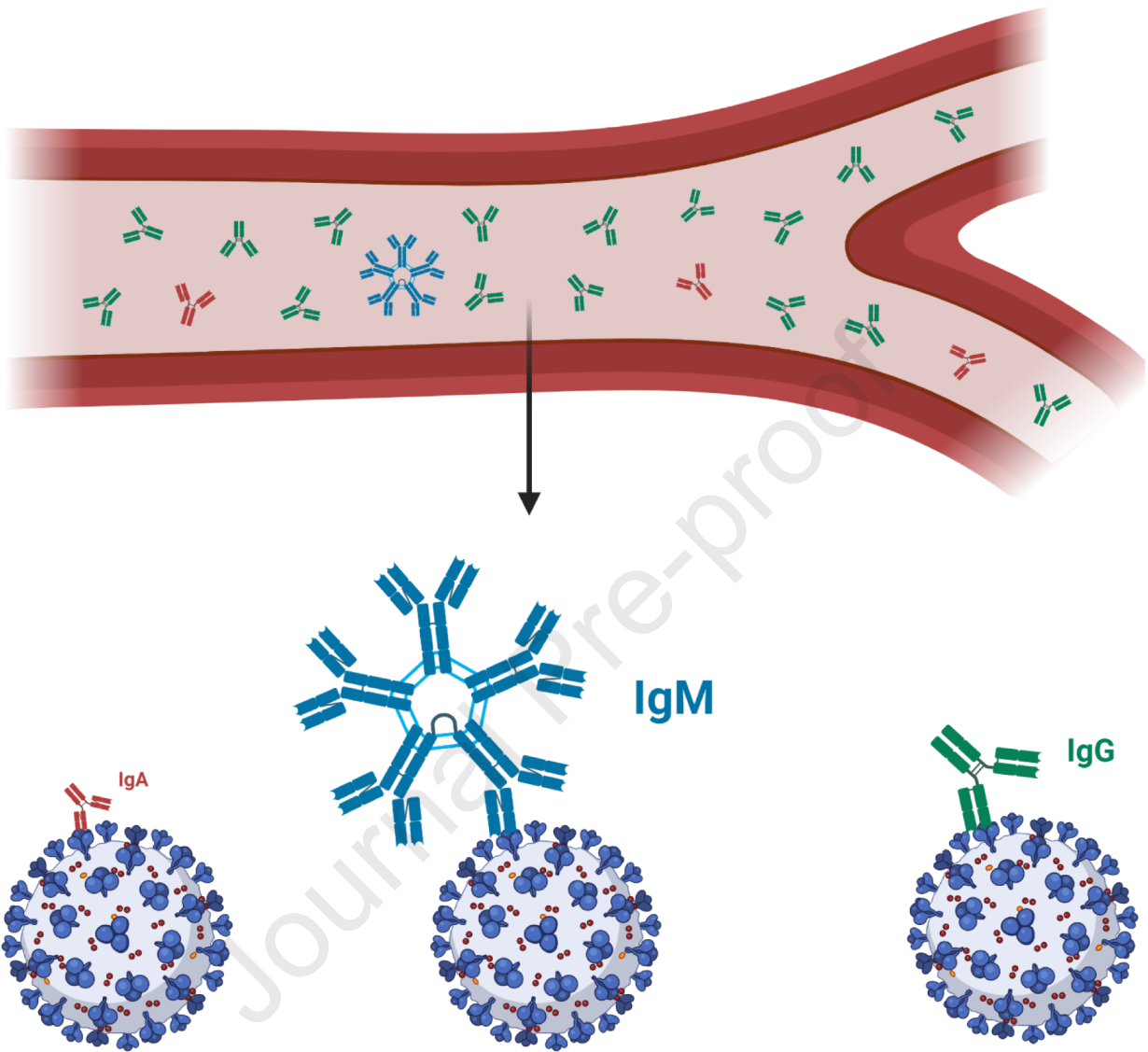
Revised Date: 5 January 2021

Accepted Date: 4 February 2021

Please cite this article as: Gasser, R., Cloutier, M., Prévost, J., Fink, C., Ducas, É., Ding, S., Dussault, N., Landry, P., Tremblay, T., Laforce-Lavoie, A., Lewin, A., Beaudoin-Bussièrès, G., Laumaea, A., Medjahed, H., Larochelle, C., Richard, J., Dekaban, G.A., Dikeakos, J.D., Bazin, R., Finzi, A., Major role of IgM in the neutralizing activity of convalescent plasma against SARS-CoV-2, *Cell Reports* (2021), doi: <https://doi.org/10.1016/j.celrep.2021.108790>.

This is a PDF file of an article that has undergone enhancements after acceptance, such as the addition of a cover page and metadata, and formatting for readability, but it is not yet the definitive version of record. This version will undergo additional copyediting, typesetting and review before it is published in its final form, but we are providing this version to give early visibility of the article. Please note that, during the production process, errors may be discovered which could affect the content, and all legal disclaimers that apply to the journal pertain.

© 2021 The Author(s).



45

46 **Summary**

47 Characterization of the humoral response to SARS-CoV-2, the etiological agent of COVID-
48 19, is essential to help control the infection. The neutralization activity of plasma from
49 COVID-19 patients decreases rapidly during the first weeks after recovery. However, the
50 specific role of each immunoglobulin isotype in the overall neutralizing capacity is still not
51 well understood. In this study, we select plasma from a cohort of COVID-19 convalescent
52 patients and selectively deplete immunoglobulin A, M or G before testing the remaining
53 neutralizing capacity of the depleted plasma. We find that depletion of immunoglobulin M is
54 associated with the most substantial loss of virus neutralization, followed by immunoglobulin
55 G. This observation may help design efficient antibody-based COVID-19 therapies and may
56 also explain the increased susceptibility to SARS-CoV-2 of autoimmune patients receiving
57 therapies that impair the production of IgM.

58

59 **Introduction**

60

61 Since its discovery in Wuhan in 2019, the causative agent of COVID-19, the SARS-CoV-2
62 virus (Zhu et al., 2020), has become a major global public health problem. A better
63 understanding of immune responses induced by SARS-CoV-2 is urgently needed to help
64 control the infection. Several studies have shown that the neutralization activity of plasma
65 from COVID-19 patients decreases rapidly during the first weeks after recovery (Beaudoin-
66 Bussi eres et al., 2020; Long et al., 2020; Pr evost et al., 2020; Robbiani et al., 2020; Seow et
67 al., 2020). Although a good correlation between the presence of Spike (S)-specific antibodies
68 and the capacity of plasma from infected individuals to neutralize viral particles was reported,
69 recent data looking at individual immunoglobulin (Ig) isotypes revealed a stronger correlation
70 between the decrease in S-specific IgM antibodies and loss of neutralization compared to S-
71 specific IgG and IgA antibodies, suggesting that IgM play an important role in the
72 neutralization activity of plasma from individuals who suffered from COVID-19 (Beaudoin-
73 Bussi eres et al., 2020; Pr evost et al., 2020). To better understand the relative contribution of
74 S-specific IgM, IgA and IgG antibodies in SARS-CoV-2 neutralization, we selectively
75 depleted each Ig isotype from plasma obtained from 25 convalescent donors and assessed the
76 impact of depletion on the capacity of the plasma to neutralize SARS-CoV-2 pseudoviral
77 particles and wild type infectious SARS-CoV-2 viral particles.

78

79 **Results**

80 Ig depletion

81 Demographic information of the 25 convalescent donors (21 males, 4 females) are presented
82 in Table 1. Each donor was sampled once between 25 and 69 days after the onset of
83 symptoms with an average time of 45 days. Selective depletion of IgM, IgA or IgG was

84 achieved by adsorption on isotype-specific ligands immobilized on Sepharose or agarose
85 beads, starting with a five-fold dilution of plasma (see details in Stars Methods). The
86 depletion protocols permitted to efficiently deplete each isotype while leaving the other
87 isotypes nearly untouched, as measured by ELISA (Fig 1A-C). Depletion of IgG had a much
88 higher impact on the total level of SARS-CoV-2 RBD antibodies than IgM and IgA depletion
89 (Fig 1D), although RBD-specific antibodies of each isotype were selectively removed by the
90 depletion as shown by their respective signals close to the background level established with
91 plasma samples collected before the outbreak of SARS-CoV-2 (red dashed line) (Fig. 1E-G).
92 The impact of IgG depletion on the level of total antibodies against the full S glycoprotein
93 expressed on 293T cells (measured by flow cytometry) was also noticeable (Fig. 1H) whereas
94 isotype-specific detection of full S antibodies by flow cytometry confirmed the efficacy of
95 selective depletion (Fig. 1I-K).

96

97 Neutralizing activity of depleted plasma

98 We then evaluated the capacity of non-depleted and isotype-depleted plasma samples to
99 neutralize pseudoviral particles expressing the S glycoprotein from SARS-CoV-2 (Prévost et
100 al., 2020) (Star Methods). Depletion of IgM, IgA or IgG all resulted in a significant decrease
101 of neutralization compared to non-depleted plasma (Fig. 2A-D). However, the loss of
102 neutralization activity was much more pronounced in IgM- and IgG-depleted plasma with a
103 5.5 and 4.5 fold decrease in mean ID_{50} compared to non-depleted plasma respectively, than in
104 IgA-depleted plasma where a 2.4 fold decrease only was observed (Fig. 2E). To evaluate
105 whether the impact of isotype depletion on neutralization could be extended beyond
106 pseudoviral particles, we tested plasma from ten donors in microneutralization experiments
107 using fully infectious SARS-CoV-2 viral particles, as described in the Star Methods. The
108 neutralizing potency of plasma was greatly reduced following IgM and IgG (4.0 and 2.8 fold

109 respectively) but not IgA (no decrease) depletion (Fig. 2F). Despite the limited number of
110 samples tested with the live virus, the impact of IgM and IgG depletion on neutralization was
111 similar to that observed with the same samples in the pseudoviral particle neutralization assay
112 (Fig. 2G-H). This data not only confirms the role of IgG in neutralizing activity of
113 convalescent plasma but also highlights the important contribution of IgM with respect to
114 neutralization activity. To further assess the consistency of our data, we compared the ID₅₀
115 obtained with pseudoviral particles and the ones obtained with full SARS-CoV-2 virions, and
116 we observed a significant correlation between the two datasets (Supp. Fig. 1).

117

118 **Discussion**

119

120 Our findings detailing the important role of IgM in the neutralizing activity of convalescent
121 plasma has several implications. First, although the therapeutic efficacy of convalescent
122 plasma for the treatment of COVID-19 patients remains to be established, it is likely that
123 neutralizing antibodies will play a role. Because SARS-CoV-2 specific IgM antibodies
124 rapidly decrease after disease onset (Beaudoin-Bussières et al., 2020; Prévost et al., 2020;
125 Robbiani et al., 2020), and the overall neutralization capacity decreases as well (Gaebler et al.,
126 2020; Grzelak et al., 2020; Seow et al., 2020) the collection of convalescent plasma with
127 maximal neutralizing activity should be performed early after disease recovery.

128 In the present work, we did not observe trends such as a more important contribution of IgM
129 in convalescent plasma taken at earlier time points (around day 30 post symptom onset) or of
130 IgG at later time points (around day 70) (Suppl Fig 2). Analysis of samples taken at much
131 later time points (for example around day 70) could nevertheless reveal a predominant role of
132 IgG in the residual neutralization activity of convalescent plasma, given the reported decrease
133 in SARS-CoV-2 IgM antibodies in most recovered patients. It should be emphasized that the

134 present study was performed with plasma samples from 25 different convalescent plasma
135 donors and not with sequential samples from a few donors. We felt that this strategy was
136 important to obtain more robust data that could be generalized to all convalescent plasma
137 collected within a few weeks after symptom onset.

138 Second, our results suggest that caution should be taken when using therapeutics that impair
139 the production of IgM. Anti-CD20 antibodies (B cell-depleting agents) are used to treat
140 several inflammatory disorders. Their use is associated with IgM deficiency in a substantial
141 number of patients, while their impact on IgG and IgA levels is more limited (Kridin and
142 Ahmed, 2020). In line with our data, recent studies reported that anti-CD20 therapy could be
143 associated with a higher susceptibility to contract SARS-CoV-2 and develop severe COVID-
144 19 (Guilpain et al., 2020; Hughes et al., 2020; Safavi et al., 2020; Schulze-Koops et al., 2020;
145 Sharmeen et al., 2020; Sormani et al., 2020). Whether this is associated to the preferential
146 depletion of IgM-producing B cells by these treatments (Looney et al., 2008) remains to be
147 shown. Nevertheless, our results suggest that IgM levels should be investigated as a
148 biomarker to stratify patients on immunosuppressive therapies at higher risk for COVID-19.

149 One limitation of this study is that it focuses on the study of the blood compartment of
150 recovered COVID-19 patients with an aim for application in convalescent plasma therapy.
151 Therefore, our data can't be generalized to the immune response happening during the early
152 stages of the disease and to the mucosal immunity in general. It has indeed been proposed
153 elsewhere that secretory IgA might play a much more significant role during the early stages
154 of the infection (Sterlin et al., 2020) and could be critical to prevent reinfection (Wang et al.,
155 2020).

156 In summary, our results extend previous observations showing a strong correlation between
157 neutralization potency and the presence of RBD-specific IgM (Beaudoin-Bussi eres et al.,
158 2020; Perera et al., 2020; Pr evost et al., 2020; Seow et al., 2020). It is intriguing that IgM

159 represents about only 5% of the total antibodies in plasma (Wang et al., 2020), yet plays such
160 an important role in SARS-CoV-2 neutralization. Whether this is due to the enhanced avidity
161 provided by its pentameric nature remains to be formally demonstrated but is in agreement
162 with recent work demonstrating that dimeric antibodies are more potent than their monomeric
163 counterpart (Wang et al., 2020). The possible establishment of long lived IgM-producing B
164 cells that might contribute to long term immunity of recovered patients has been suggested
165 (Brouwer et al., 2020; Newell et al., 2020). However, how plasma neutralization evolves over
166 prolonged periods of time and the specific role of IgM in this activity remains to be
167 determined.

168

169 **Acknowledgments**

170 We thank Stefan Pöhlmann for kindly providing the plasmid expressing the SARS-CoV-2 S
171 glycoprotein. This work was supported by “Ministère de l’Économie et de l’Innovation du
172 Québec, Programme de soutien aux organismes de recherche et d’innovation”, by the
173 Fondation du CHUM, by the Canada’s COVID-19 Immunity Task Force (CITF), in
174 collaboration with the Canadian Institutes of Health Research (CIHR) and a CIHR foundation
175 grant #352417 to A.F. Funding was also provided by an operating grant from CIHR from the
176 Canadian 2019 Novel Coronavirus (COVID-19) Rapid Research Funding Opportunity
177 (FRN440388 to JDD and GAD) and an Infrastructure Grant from CFI for the Imaging
178 Pathogens for Knowledge Translation (ImPaKT) Facility (#36287 to JDD and GAD). A.F. is
179 the recipient of a Canada Research Chair on Retroviral Entry # RCHS0235 950-232424. R.G.
180 is supported by a MITACS Accélération postdoctoral fellowship. J.P. is supported by a CIHR
181 graduate fellowship. The graphical abstract has been generated with BioRender website.

182

183

184

185

186 Author Contributions

187 R.G., M.C., J.P., R.B. and A.F. designed the studies. R.G. and S.D. performed neutralization
188 experiments with pseudoviral particles. J.P. performed flow cytometry experiments. C.F.,
189 G.A.D. and J.D.D. performed microneutralization assays with infectious wildtype SARS-
190 CoV-2 and analysed the results. M.C., E.D., N.D., P.L., A.L.L. and T.T. depleted plasma
191 samples and performed the ELISA. J.R. provided new reagents. A.L. performed statistical
192 analysis. C.L. provided scientific and clinical input. R.G., M.C., R.B. and A.F. wrote the
193 manuscript with inputs from others. Every author has read, edited and approved the final
194 manuscript.

195

196 Competing interests

197 The authors declare no-competing interests

198

199

200 Figure Legends

201

202 Figure 1. IgM, IgA and IgG depletion in plasma samples from convalescent donors.

203 (A-C) Efficacy of the specific isotype depletion assessed by ELISA for total IgM, IgA and
204 IgG. All plasma samples were diluted 5-fold prior to depletion; (A) IgM concentration in non-
205 depleted, IgM-depleted, IgA-depleted and IgG-depleted plasmas, measured using an anti-
206 human IgM (μ -chain specific) as capture antibody; (B) IgA concentration measured on the
207 same plasmas using anti-human IgA (α -chain specific); (C) IgG concentration measured
208 using anti-human IgG (γ -chain specific). (D-G) Efficacy of SARS-CoV-2 specific antibody
209 depletion assessed by SARS-CoV-2 RBD ELISA; (D) Level of total (pan-Ig) anti-SARS-
210 CoV-2 RBD-specific antibodies in non-depleted, IgM-depleted, IgA depleted and IgG-
211 depleted plasmas; (E) Level of IgM-specific anti-RBD; (F) Level of IgA-specific anti-RBD;
212 (G) Level of IgG-specific anti-RBD. (H-K) Efficacy of full S glycoprotein-specific antibody
213 depletion measured by flow cytometry; (H) Level of total (pan-Ig) anti-SARS-CoV-2 S-
214 specific antibodies in non-depleted, IgM-depleted, IgA-depleted and IgG-depleted plasmas;
215 (I) Level of IgM-specific anti-S; (J) Level of IgA-specific anti-S; (K) Level of IgG-specific
216 anti-S. Red dashed lines represent the average signal given by negative controls taken from
217 non-infected patients. Asterisks indicate the level of statistical significance obtained by a
218 Dunn's test; **** $p < 0.0001$.

219

220 Figure 2. Role of IgM, IgA and IgG in neutralization.

221 (A) Comparison of the SARS-CoV-2 pseudoviral inhibitory dilution (ID_{50}) of all plasma
222 samples. (B-D) ID_{50} of plasma from each convalescent donor before and after (B) IgM, (C)
223 IgA and (D) IgG depletion. (E) Fold decrease (isotype-depleted versus non-depleted plasma)
224 in ID_{50} measured by SARS-CoV-2 pseudoviral particle neutralization. (F-G)

225 Microneutralization assay using infectious wild type SARS-CoV-2 performed on non-
 226 depleted and isotype-depleted plasma from 10 donors, (F) mean percentage of infection and
 227 (G) ID₅₀ observed with plasma from the 10 donors. (H) ID₅₀ obtained using the pseudoviral
 228 particle neutralization assay for the samples in (F-G). Asterisks indicate the level of statistical
 229 significance obtained by a Wilcoxon signed rank test, n.s. not significant; *p<0.05; **p<0.01;
 230 ***p<0.001; ****p<0.0001.

231

232 **Table 1. COVID convalescent plasma donor's characteristics**

	All donors	Males	Females
Donors (n)	25	21	4
Average age ± SD [range]	47 ± 16 [20-69]	49 ± 17 [20-69]	40 ± 14 [29-60]
Age (median)	50	51	34.5
Average time (days) between symptoms onset and donation (median [range])	45 [25-69]	47 [25-69]	40 [27-56]

233

234

235 STAR Methods**236 Lead Contact**

237 Further information and requests for resources and reagents should be directed to and will be
238 fulfilled by the Lead Contact (andres.finzi@umontreal.ca).

239

240 Materials availability

241 All unique reagents generated during this study are available from the Lead contact without
242 restriction.

243

244 Data and Code Availability

245 This study did not generate new code.

246

247 Experimental model and subjects detail

248

249 Ethics statement

250 All work was conducted in accordance with the Declaration of Helsinki in terms of informed
251 consent and approval by an appropriate Ethics Review board. Convalescent plasmas were
252 obtained from donors who consented to participate in this research project at CHUM (19.381)
253 and at Héma-Québec (REB # 2020-004). The donors met all donor eligibility criteria:
254 previous confirmed COVID-19 infection and complete resolution of symptoms for at least 14
255 days.

256

257 Human subjects

258 No specific criteria such as number of patients (sample size), clinical or demographic were
259 used for inclusion, beyond PCR confirmed SARS-CoV-2 infection in adults.

260

261 Plasmids

262 The plasmids expressing the human coronavirus Spike of SARS-CoV-2 was kindly provided
263 by Stefan Pöhlmann and was previously reported (Hoffmann et al., 2020). The pNL4.3 R-E-
264 Luc was obtained from NIH AIDS Reagent Program. The codon-optimized RBD sequence
265 (encoding residues 319-541) fused to a C-terminal hexahistidine tag was cloned into the
266 pcDNA3.1(+) expression vector and was reported elsewhere (Beaudoin-Bussièrès et al.,
267 2020). The vesicular stomatitis virus G (VSV-G)-encoding plasmid (pSVCMV-IN-VSV-G)
268 was previously described (Lodge et al., 1997).

269

270 Cell lines

271 293T human embryonic kidney cells (obtained from ATCC) and Vero E6 cells (ATCC CRL-
272 1586™) were maintained at 37°C under 5% CO₂ in Dulbecco's modified Eagle's medium
273 (DMEM) (Wisent) containing 5% fetal bovine serum (VWR), 100 UI/ml of penicillin and
274 100µg/ml of streptomycin (Wisent). The 293T-ACE2 cell line has been generated by us and
275 was previously reported (Prévost et al., 2020). For the generation of 293T cells stably
276 expressing SARS-CoV-2 Spike the same technique than previously described has been used
277 (Prévost et al., 2020) : VSV-G pseudotyped lentivirus packaging the SARS-CoV-2 Spike
278 gene was produced in 293T using a third-generation lentiviral vector system. Briefly, 293T
279 cells were co-transfected with two packaging plasmids (pLP1 and pLP2), an envelope plasmid
280 (pSVCMV-IN-VSV-G) and a lentiviral transfer plasmid coding for a GFP-tagged SARS-
281 CoV-2 Spike (pLV-SARS-CoV-2 S C-GFPSpark tag) (SinoBiological). Supernatant
282 containing lentiviral particles was used to infect 293T cells in presence of 5µg/mL polybrene.
283 The 293T cells stably expressing SARS-CoV-2 Spike (GFP+) were sorted by flow cytometry.
284 SARS-CoV-2 expression was confirmed using the CR3022 mAb and plasma from SARS-
285 CoV-2-infected individuals.

286

287 Methods detail

288

289 Isotype depletion

290 Selective depletion of IgM, IgA or IgG was done by adsorption on isotype-specific ligands
291 immobilized on sepharose or agarose beads starting with a five-fold dilution of plasma in
292 PBS. IgG and IgA antibodies were depleted from plasma obtained from 25 recovered
293 COVID-19 patient using Protein G HP Spintrap (Cytiva, formerly GE Healthcare Life
294 Sciences, Buckinghamshire, UK) and Peptide M / Agarose (InvivoGen, San Diego, CA),
295 respectively, according to the manufacturer's instructions with the exception that no elution
296 step for the recovery of the targeted antibodies was done, because the elution of bound
297 antibodies requires exposure to denaturing conditions (for example acidic pH) which,
298 according to several reports in the literature, could alter their biological activity (Bergmann-
299 Leitner et al., 2008; Dimitrov et al., 2007; St-Amour et al., 2009). For IgM depletion, anti-
300 human IgM (μ -chain specific, Sigma, St.Louis, MO) was covalently coupled to NHS HP
301 SpinTrap (Cytiva, formerly GE Healthcare) at 815 $\mu\text{g}/\text{mL}$ of matrix. Depletion was performed
302 according to the manufacturer's instructions with the exception that no elution step for the
303 recovery of the targeted isotype was done. All non-depleted and isotype-depleted samples
304 were filtered on a 0.22 μm Millex GV filter (SLGV013SL, Millipore, Burlington, MA) to
305 ensure sterility for the virus capture and neutralization assays.

306

307 Immunoglobulin isotype ELISA

308 To assess the extent of IgM, IgG and IgA depletion, ELISA were performed on non-depleted
309 as well as IgM-, IgA- and IgG-depleted plasma samples. Each well of a 96-well microplate
310 was filled with either goat anti-human IgM (μ -chain specific) at 5 $\mu\text{g}/\text{mL}$, goat anti-human

311 serum IgA (α -chain specific) at 0.3 $\mu\text{g}/\text{mL}$ or goat anti-human IgG (γ -chain specific) at 5
312 $\mu\text{g}/\text{mL}$ (all from Jackson ImmunoResearch Laboratories, Inc., West Grove, PA). Microtiter
313 plates were sealed and stored overnight at 2- 8°C. After four (IgA) to six (IgM and IgG)
314 washes with H_2O -0.1% Tween 20 (Sigma), 200 μL of blocking solution (10 mmol/L
315 phosphate buffer, pH 7.4, containing 0.85% NaCl, 0.25% Hammerstein casein (EMD
316 Chemicals Inc., Gibbstown, NJ,) were added to each well to block any remaining binding
317 sites. The blocking solution for the IgG and IgM ELISA also contained 0.05% Tween 20.
318 After 0.5 (IgA) to 1h (IgM and IgG) incubation at 37°C and washes, samples and the standard
319 curves (prepared with human calibrated standard serum, Cedarlane, Burlington, Canada) were
320 added to the plates in triplicates. Plates were incubated for 1h at 37°C. After washes, 100 μL
321 of either goat anti-human IgA+G+M (H+L) HRP conjugate (1/30 000), goat anti-human IgG
322 (H+L) HRP conjugate (1/30 000), goat anti-human IgM (μ -chain specific) HRP conjugate
323 (1/10 000) or goat anti-human IgA (α -chain specific) HRP conjugate (1/10 000) (all from
324 Jackson ImmunoResearch Laboratories, Inc.) were added and samples were incubated at 37°C
325 for 1h. Wells were washed and bound antibodies were detected by the addition of 100 μL of
326 3,3',5,5'-tetramethylbenzimidine (TMB, ScyTek Laboratories, Logan, UT). The enzymatic
327 reaction was stopped by the addition of 100 μL 1 N H_2SO_4 and the absorbance was measured
328 at 450/630 nm within 5 minutes.

329

330 SARS-CoV-2 RBD ELISA

331 The presence of SARS-CoV-2 RBD-specific antibodies in the plasma from 25 recovered
332 COVID-19 patients before and after depletion was measured using an ELISA adapted from a
333 recently described protocol (Beaudoin-Bussières et al., 2020; Perreault et al., 2020; Prévost et
334 al., 2020). The plasmid encoding for SARS-CoV-2 RBD was synthesized commercially
335 (Genscript, Piscataway, NJ, USA) (Amanat et al., 2020a). Recombinant RBD proteins were

336 produced in transfected FreeStyle 293F cells (Invitrogen, Carlsbad, CA, USA) and purified by
337 nickel affinity chromatography. Recombinant RBD was diluted to 2.5 µg/mL in PBS (Thermo
338 Fisher Scientific, Waltham, MA, USA) and 100 µl of the dilution was distributed in the wells
339 of flat-bottom 96-well microplates (Immulon 2HB; Thermo Scientific). The plates were
340 placed overnight at 2-8°C for antigen adsorption. For the assay, the plates were emptied and a
341 volume of 300 µl/well of blocking buffer (PBS-0.1% Tween (Sigma)-2% BSA (Sigma)) was
342 added. The microplates were incubated for one hour at room temperature (RT) followed by
343 washing four times (ELx405 microplate washer, Bio-Tek) with 300 µL/well of washing
344 solution (PBS-0.1% Tween). Because the reaction is time sensitive, samples, negative and
345 positive controls were prepared in triplicates in a plate, then transferred in the RBD coated
346 plate by reverse multi-pipetting. The negative control was prepared from a pool of 23 COVID
347 negative plasmas while the positive control was a characterized plasma from a recovered
348 patient. After transfer, the plates were incubated for 60 minutes at 20-24°C. After four
349 washes, 100 µL of either goat anti-human IgA+G+M (H+L) HRP conjugate (1/30 000) for the
350 detection of all isotypes, goat anti-human IgM (µ-chain specific) HRP conjugate (1/15 000),
351 F(ab')₂ fragment goat anti-human IgA (α-chain specific) HRP conjugate (1/4500) (all from
352 Jackson Immunosearch Laboratories, Inc.) or goat anti-human IgG (γ-chain specific) HRP
353 conjugate (1/50 000) (Invitrogen) were added and samples were incubated at 20-24°C for 60
354 minutes. Wells were washed four times and bound antibodies were detected by the addition of
355 100 µL of 3,3',5,5'-tetramethylbenzimidine (ScyTek Laboratories). The enzymatic reaction
356 was stopped by the addition of 100 µL 1 N H₂SO₄ and the absorbance was measured at
357 450/630 nm within 5 minutes.

358

359 Flow cytometry analysis of cell-surface staining

360 293T cells stably expressing SARS-CoV-2 Spike with a C-GFP tag (293T-Spike) were mixed
361 at a 1:1 ratio with non-transduced 293T cells and were stained with plasma from SARS-CoV-
362 2-infected individuals (1:250 dilution). Plasma binding to cell-surface Spike was revealed
363 using fluorescent secondary antibodies able to detect all Ig isotypes (anti-human
364 IgM+IgG+IgA; Jackson ImmunoResearch Laboratories, Inc.) or specific to IgG isotype
365 (Biolegend), IgM isotype (Jackson ImmunoResearch Laboratories, Inc.) or IgA isotype
366 (Jackson ImmunoResearch Laboratories, Inc.). The living cell population was gated on the
367 basis of a viability dye staining (Aqua Vivid, Invitrogen). Samples were acquired on a LSRII
368 cytometer (BD Biosciences, Mississauga, ON, Canada) and data analysis was performed
369 using FlowJo v10.5.3 (Tree Star, Ashland, OR). The signal obtained with 293T (GFP-
370 population) was subtracted from the signal obtained with 293T-Spike (GFP+ population) to
371 remove unspecific signal.

372

373 Neutralization assay using pseudoviral particles

374 Target cells were infected with single-round luciferase-expressing lentiviral particles as
375 described previously (Prévost et al., 2020). Briefly, 293T cells were transfected by the
376 calcium phosphate method with the lentiviral vector pNL4.3 R-E- Luc (NIH AIDS Reagent
377 Program) and a plasmid encoding for SARS-CoV-2 Spike at a ratio of 5:4. Two days post-
378 transfection, cell supernatants were harvested and stored at -80°C until use. 293T-ACE2
379 target cells were seeded at a density of 1×10^4 cells/well in 96-well luminometer-compatible
380 tissue culture plates (Perkin Elmer) 24h before infection. Recombinant viruses in a final
381 volume of 100 μl were incubated with the indicated plasma dilutions (1/50; 1/250; 1/1250;
382 1/6250; 1/31 250) for 1h at 37°C and were then added to the target cells followed by
383 incubation for 48h at 37°C ; cells were lysed by the addition of 30 μl of passive lysis buffer
384 (Promega) followed by one freeze-thaw cycle. An LB941 TriStar luminometer (Berthold

385 Technologies) was used to measure the luciferase activity of each well after the addition of
386 100µl of luciferin buffer (15mM MgSO₄, 15mM KPO₄ [pH 7.8], 1mM ATP, and 1mM
387 dithiothreitol) and 50µl of 1mM d-luciferin potassium salt (Prolume). The neutralization half-
388 maximal inhibitory dilution (ID₅₀) represents the sera dilution to inhibit 50% of the infection
389 of 293T-ACE2 cells by recombinant viruses.

390

391 Microneutralization assay using live SARS-CoV-2 viral particles

392 A microneutralization assay for SARS-CoV-2 serology was performed as previously
393 described (Amanat et al., 2020b). The assay was conducted with the person blinded to the
394 sample identity. Experiments were conducted with the SARS-CoV-2 USA-WA1/2020 virus
395 strain. This reagent was deposited by the Centers for Disease Control and Prevention and
396 obtained through BEI Resources, NIAID, NIH: SARS-Related Coronavirus 2, Isolate USA-
397 WA1/2020, NR-52281. One day prior to infection, 2×10^4 Vero E6 cells were seeded per well
398 of a 96 well flat bottom plate and incubated overnight (37°C/5% CO₂) to permit Vero E6 cell
399 adherence. On the day of infection, all plasma samples were heat inactivated at 56°C for one
400 hour. Non-depleted plasma from each donor was also included in this assay. Plasma dilutions
401 were performed in a separate 96 well culture plate using MEM supplemented with penicillin
402 (100 U/mL), streptomycin (100 µg/mL), HEPES, L-Glutamine (0.3 mg/mL), 0.12% sodium
403 bicarbonate, 2% FBS (all from Thermo Fisher Scientific) and 0.24% BSA (EMD Millipore
404 Corporation). Plasma dilutions ranged from 1:50 to 1:31 250. In a Biosafety Level 3
405 laboratory (ImPaKT Facility, Western University), 10^3 TCID₅₀/mL SARS-CoV-2 USA-
406 WA1/2020 virus strain was prepared in MEM + 2% FBS and combined with an equivalent
407 volume of respective plasma dilution for one hour at room temperature. After this incubation,
408 all media was removed from the 96 well plate seeded with Vero E6 cells and virus:plasma
409 mixtures were added to each respective well at a volume corresponding to 600 TCID₅₀ per

410 well and incubated for one hour further at 37°C. Both virus only and media only (MEM + 2%
411 FBS) conditions were included in this assay. All virus:plasma supernatants were removed
412 from wells without disrupting the Vero E6 monolayer. Each plasma dilution (100 µL) was
413 added to its respective Vero E6-seeded well in addition to an equivalent volume of MEM +
414 2% FBS and was then incubated for 48 hours. Media was then discarded and replaced with
415 10% formaldehyde for 24 hours to cross-link Vero E6 monolayer. Formaldehyde was
416 removed from wells and subsequently washed with PBS. Cell monolayers were permeabilized
417 for 15 minutes at room temperature with PBS + 0.1% Triton X-100 (BDH Laboratory
418 Reagents), washed with PBS and then incubated for one hour at room temperature with PBS +
419 3% non-fat milk. An anti-mouse SARS-CoV-2 nucleocapsid protein (Clone 1C7, Bioss
420 Antibodies) primary antibody solution was prepared at 1 µg/mL in PBS + 1% non-fat milk
421 and added to all wells for one hour at room temperature. Following extensive washing with
422 PBS, an anti-mouse IgG HRP secondary antibody solution was formulated in PBS + 1% non-
423 fat milk. One hour post-room temperature incubation, wells were washed with PBS,
424 SIGMAFAST™ OPD developing solution (Millipore Sigma) was prepared as per
425 manufacturer's instructions and added to each well for 12 minutes. Dilute HCl (3.0 M) was
426 added to quench the reaction and the optical density at 490 nm of the culture plates was
427 immediately measured using a Synergy LX multi-mode reader and Gen5™ microplate reader
428 and imager software (BioTek®).

429

430 **Quantification and statistical analysis**

431

432 Statistical analysis

433 Statistics were analyzed using GraphPad Prism version 8.0.2 (GraphPad, San Diego, CA,
434 (USA). Every data set was tested for statistical normality and this information was used to

435 apply the appropriate (parametric or nonparametric) statistical test. P values <0.05 were
436 considered significant; significance values are indicated as $*p<0.05$; $**p<0.01$; $***p<0.001$;
437 $****p<0.0001$.

438

Journal Pre-proof

439 **References**

- 440 Amanat, F., Stadlbauer, D., Strohmeier, S., Nguyen, T.H.O., Chromikova, V., McMahon, M.,
441 Jiang, K., Arunkumar, G.A., Jurczynszak, D., Polanco, J., et al. (2020a). A serological assay to
442 detect SARS-CoV-2 seroconversion in humans. *Nat. Med.* 26, 1033–1036.
- 443 Amanat, F., White, K.M., Miorin, L., Strohmeier, S., McMahon, M., Meade, P., Liu, W.-C.,
444 Albrecht, R.A., Simon, V., Martinez-Sobrido, L., et al. (2020b). An In Vitro
445 Microneutralization Assay for SARS-CoV-2 Serology and Drug Screening. *Curr. Protoc.*
446 *Microbiol.* 58, e108.
- 447 Beaudoin-Bussièrès, G., Laumaea, A., Anand, S.P., Prévost, J., Gasser, R., Goyette, G.,
448 Medjahed, H., Perreault, J., Tremblay, T., Lewin, A., et al. (2020). Decline of Humoral
449 Responses against SARS-CoV-2 Spike in Convalescent Individuals. *MBio* 11.
- 450 Bergmann-Leitner, E.S., Mease, R.M., Duncan, E.H., Khan, F., Waitumbi, J., and Angov, E.
451 (2008). Evaluation of immunoglobulin purification methods and their impact on quality and
452 yield of antigen-specific antibodies. *Malar. J.* 7, 129.
- 453 Brouwer, P.J.M., Caniels, T.G., van der Straten, K., Snitselaar, J.L., Aldon, Y., Bangaru, S.,
454 Torres, J.L., Okba, N.M.A., Claireaux, M., Kerster, G., et al. (2020). Potent neutralizing
455 antibodies from COVID-19 patients define multiple targets of vulnerability. *Science*.
- 456 Dimitrov, J.D., Lacroix-Desmazes, S., Kaveri, S.V., and Vassilev, T.L. (2007). Transition
457 towards antigen-binding promiscuity of a monospecific antibody. *Mol. Immunol.* 44, 1854–
458 1863.
- 459 Gaebler, C., Wang, Z., Lorenzi, J.C.C., Muecksch, F., Finkin, S., Tokuyama, M., Ladinsky,
460 M., Cho, A., Jankovic, M., Schaefer-Babajew, D., et al. (2020). Evolution of Antibody
461 Immunity to SARS-CoV-2. *BioRxiv* 2020.11.03.367391.
- 462 Grzelak, L., Velay, A., Madec, Y., Gallais, F., Staropoli, I., Schmidt-Mutter, C., Wendling,
463 M.-J., Meyer, N., Planchais, C., Rey, D., et al. (2020). Sex differences in the decline of
464 neutralizing antibodies to SARS-CoV-2. *MedRxiv* 2020.11.12.20230466.
- 465 Guilpain, P., Le Bihan, C., Foulongne, V., Taourel, P., Pansu, N., Maria, A.T.J., Jung, B.,
466 Larcher, R., Klouche, K., and Le Moing, V. (2020). Rituximab for granulomatosis with
467 polyangiitis in the pandemic of covid-19: lessons from a case with severe pneumonia. *Ann.*
468 *Rheum. Dis.*
- 469 Hoffmann, M., Kleine-Weber, H., Schroeder, S., Krüger, N., Herrler, T., Erichsen, S.,
470 Schiergens, T.S., Herrler, G., Wu, N.-H., Nitsche, A., et al. (2020). SARS-CoV-2 Cell Entry
471 Depends on ACE2 and TMPRSS2 and Is Blocked by a Clinically Proven Protease Inhibitor.
472 *Cell* 181, 271-280.e8.
- 473 Hughes, R., Pedotti, R., and Koendgen, H. (2020). COVID-19 in persons with multiple
474 sclerosis treated with ocrelizumab – A pharmacovigilance case series. *Mult. Scler. Relat.*
475 *Disord.* 42, 102192.
- 476 Kridin, K., and Ahmed, A.R. (2020). Post-rituximab immunoglobulin M (IgM)
477 hypogammaglobulinemia. *Autoimmun. Rev.* 19, 102466.

- 478 Lodge, R., Lalonde, J.P., Lemay, G., and Cohen, E.A. (1997). The membrane-proximal
479 intracytoplasmic tyrosine residue of HIV-1 envelope glycoprotein is critical for basolateral
480 targeting of viral budding in MDCK cells. *EMBO J.* *16*, 695–705.
- 481 Long, Q.-X., Tang, X.-J., Shi, Q.-L., Li, Q., Deng, H.-J., Yuan, J., Hu, J.-L., Xu, W., Zhang,
482 Y., Lv, F.-J., et al. (2020). Clinical and immunological assessment of asymptomatic SARS-
483 CoV-2 infections. *Nat. Med.* *26*, 1200–1204.
- 484 Looney, R.J., Srinivasan, R., and Calabrese, L.H. (2008). The effects of rituximab on
485 immunocompetency in patients with autoimmune disease. *Arthritis Rheum.* *58*, 5–14.
- 486 Newell, K.L., Clemmer, D.C., Cox, J.B., Kayode, Y.I., Zoccoli-Rodriguez, V., Taylor, H.E.,
487 Endy, T.P., Wilmore, J.R., and Winslow, G. (2020). Switched and unswitched memory B
488 cells detected during SARS-CoV-2 convalescence correlate with limited symptom duration.
489 MedRxiv 2020.09.04.20187724.
- 490 Perera, R.A., Mok, C.K., Tsang, O.T., Lv, H., Ko, R.L., Wu, N.C., Yuan, M., Leung, W.S.,
491 Chan, J.M., Chik, T.S., et al. (2020). Serological assays for severe acute respiratory syndrome
492 coronavirus 2 (SARS-CoV-2), March 2020. *Eurosurveillance* *25*, 2000421.
- 493 Perreault, J., Tremblay, T., Fournier, M.-J., Drouin, M., Beaudoin-Bussièrès, G., Prévost, J.,
494 Lewin, A., Bégin, P., Finzi, A., and Bazin, R. (2020). Waning of SARS-CoV-2 RBD
495 antibodies in longitudinal convalescent plasma samples within four months after symptom
496 onset. *Blood*.
- 497 Prévost, J., Gasser, R., Beaudoin-Bussièrès, G., Richard, J., Duerr, R., Laumaea, A., Anand,
498 S.P., Goyette, G., Benlarbi, M., Ding, S., et al. (2020). Cross-sectional evaluation of humoral
499 responses against SARS-CoV-2 Spike. *Cell Rep. Med.* 100126.
- 500 Robbiani, D.F., Gaebler, C., Muecksch, F., Lorenzi, J.C.C., Wang, Z., Cho, A., Agudelo, M.,
501 Barnes, C.O., Gazumyan, A., Finkin, S., et al. (2020). Convergent antibody responses to
502 SARS-CoV-2 in convalescent individuals. *Nature* *584*, 437–442.
- 503 Safavi, F., Nourbakhsh, B., and Azimi, A.R. (2020). B-cell depleting therapies may affect
504 susceptibility to acute respiratory illness among patients with multiple sclerosis during the
505 early COVID-19 epidemic in Iran. *Mult. Scler. Relat. Disord.* *43*, 102195.
- 506 Schulze-Koops, H., Krueger, K., Vallbracht, I., Hasseli, R., and Skapenko, A. (2020).
507 Increased risk for severe COVID-19 in patients with inflammatory rheumatic diseases treated
508 with rituximab. *Ann. Rheum. Dis.*
- 509 Seow, J., Graham, C., Merrick, B., Acors, S., Pickering, S., Steel, K.J.A., Hemmings, O.,
510 O’Byrne, A., Kouphou, N., Galao, R.P., et al. (2020). Longitudinal observation and decline of
511 neutralizing antibody responses in the three months following SARS-CoV-2 infection in
512 humans. *Nat. Microbiol.* *5*, 1598–1607.
- 513 Sharmeen, S., Elghawy, A., Zarlusht, F., and Yao, Q. (2020). COVID-19 in rheumatic disease
514 patients on immunosuppressive agents. *Semin. Arthritis Rheum.* *50*, 680–686.
- 515 Sormani, M.P., De Rossi, N., Schiavetti, I., Carmisciano, L., Cordioli, C., Moiola, L.,
516 Radaelli, M., Immovilli, P., Capobianco, M., Trojano, M., et al. (2020). Disease Modifying

- 517 Therapies and COVID-19 Severity in Multiple Sclerosis (Rochester, NY: Social Science
518 Research Network).
- 519 St-Amour, I., Laroche, A., Bazin, R., and Lemieux, R. (2009). Activation of cryptic IgG
520 reactive with BAFF, amyloid beta peptide and GM-CSF during the industrial fractionation of
521 human plasma into therapeutic intravenous immunoglobulins. *Clin. Immunol. Orlando Fla*
522 *133*, 52–60.
- 523 Sterlin, D., Fadlallah, J., Adams, O., Fieschi, C., Parizot, C., Dorgham, K., Rajkumar, A.,
524 Autaa, G., El-Kafsi, H., Charuel, J.-L., et al. (2020). Human IgA binds a diverse array of
525 commensal bacteria. *J. Exp. Med.* *217*.
- 526 Wang, Z., Lorenzi, J.C.C., Muecksch, F., Finkin, S., Viant, C., Gaebler, C., Cipolla, M.,
527 Hoffmann, H.-H., Oliveira, T.Y., Oren, D.A., et al. (2020). Enhanced SARS-CoV-2
528 neutralization by dimeric IgA. *Sci. Transl. Med.*
- 529 Zhu, N., Zhang, D., Wang, W., Li, X., Yang, B., Song, J., Zhao, X., Huang, B., Shi, W., Lu,
530 R., et al. (2020). A Novel Coronavirus from Patients with Pneumonia in China, 2019. *N.*
531 *Engl. J. Med.*
- 532

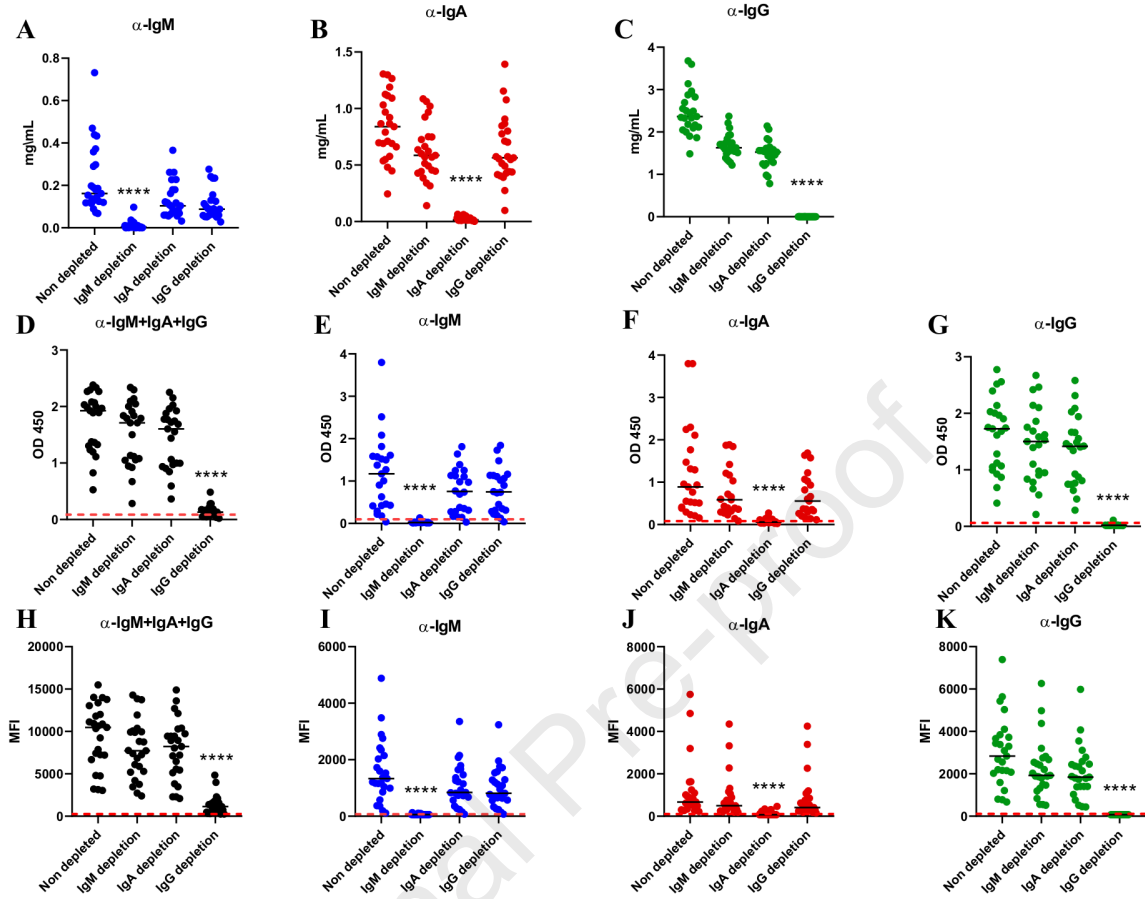
Highlights

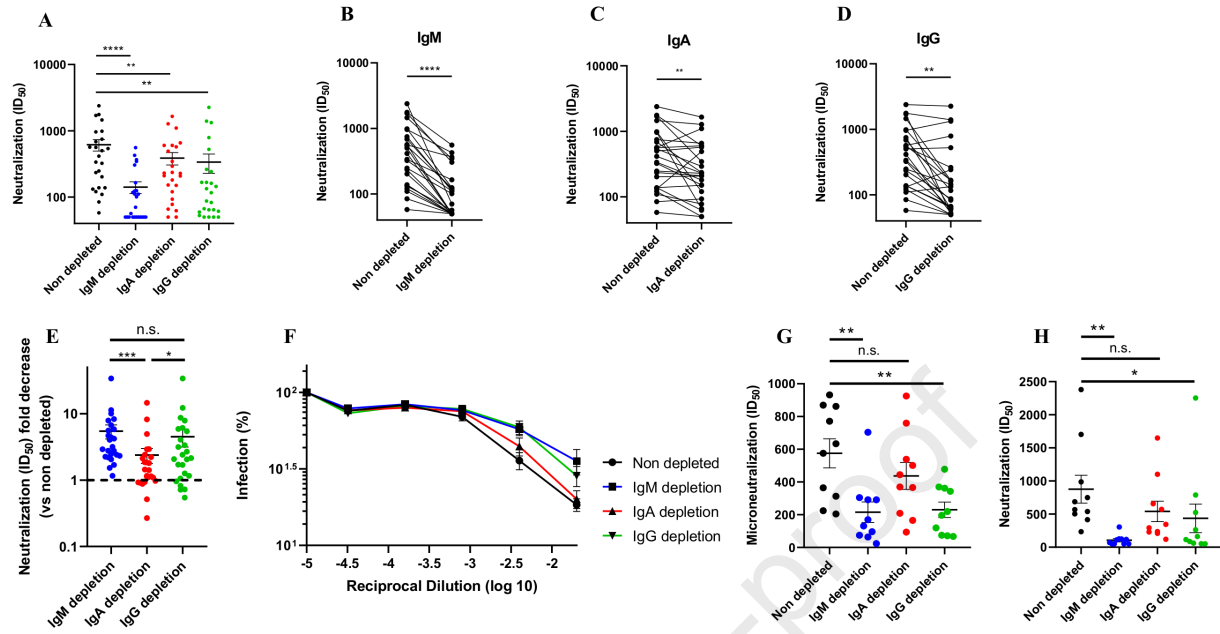
- IgM plays a major role in the capacity of convalescent plasma to neutralize SARS-CoV-2
- IgM represents about only 5% of total antibodies in plasma
- The pentameric nature of IgM might increase its avidity for trimeric SARS-CoV-2 spike

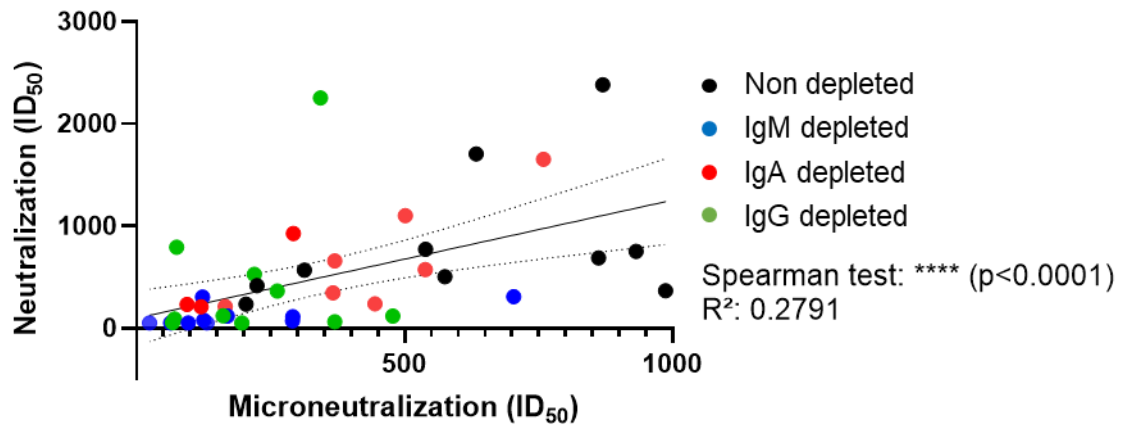
eTOC Blurb

Gasser et al. highlight the importance of IgM in the capacity of plasma from convalescent donors to neutralize SARS-CoV-2.

Journal Pre-proof

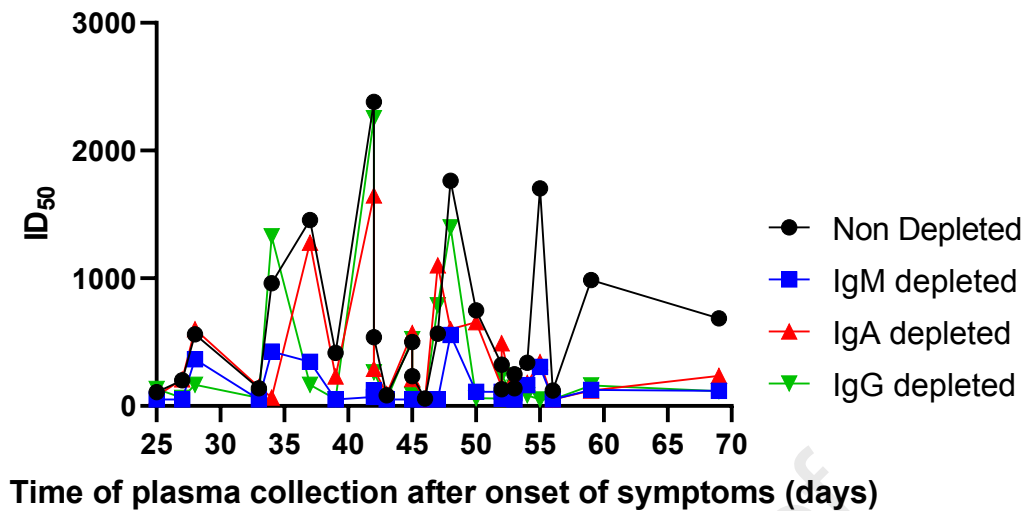






Supplemental Figure 1. Correlation between the neutralizing capacity of the ten convalescent plasma tested by pseudoviral particle neutralization or microneutralization with infectious wild type SARS-CoV-2 virus - Related to Figure 2.

Spearman correlation and linear regression fitting between the ID₅₀ obtained by microneutralization and pseudoviral particles neutralization assays. Dashed lines indicate the 95% confidence interval of the linear regression fitting. Non-depleted plasmas are shown in black, IgM-depleted in blue, IgA-depleted in red and IgG-depleted in green. Asterisks indicate the level of statistical significance obtained by a Wilcoxon signed rank test; ****p<0.0001.



Supplemental Figure 2. Neutralizing capacity of convalescent plasma as a function of the time of collection after symptoms onset – Related to Table 1.

ID₅₀ obtained by neutralization experiments with pseudoviral particles were plotted as a function of the time of plasma collection after onset of symptoms. Therefore, each time point represents a single patient, the earliest plasma collection took place 25 days after the onset of symptoms of the corresponding patient and the latest, 69 days after the onset of symptoms. Non-depleted plasmas are shown in black, IgM-depleted in blue, IgA-depleted in red and IgG-depleted in green.